Vismate: Interactive Visual Analysis of Station-Based Observation Data on Climate Changes

Jie Li, Kang Zhang, and Zhao-Peng Meng

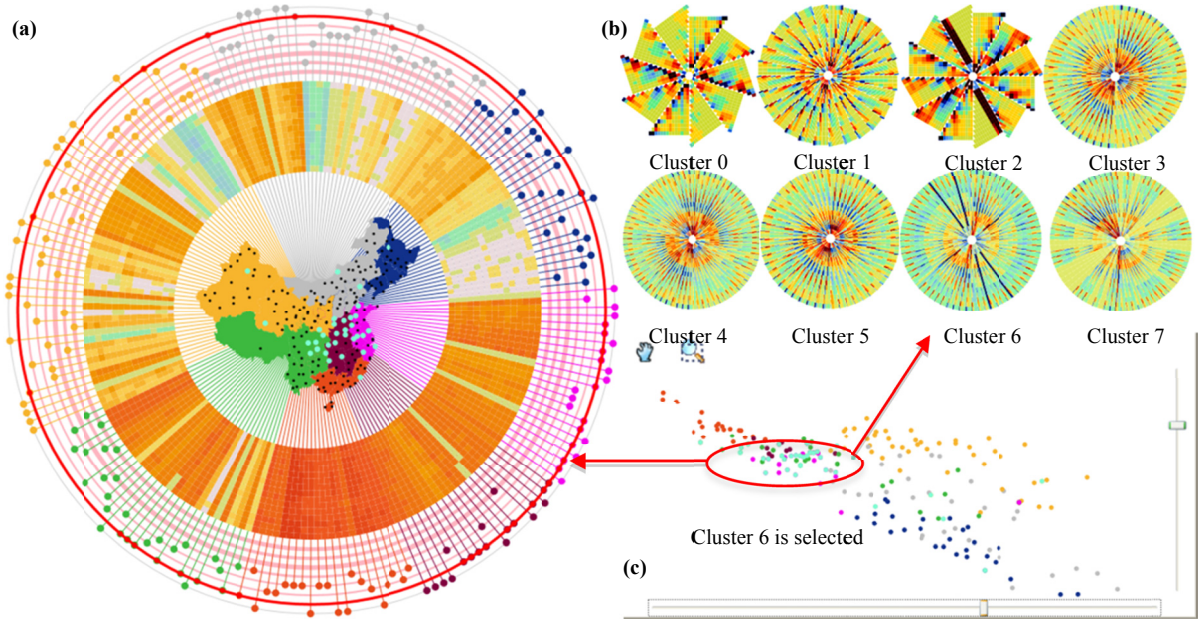

Fig. 1. Visualizing the climate change in China during the period of 1975 - 1989 based on the surface observation data. (a) Global Radial Map used to visualize the overall state. From the center: a map, a sector-based ring-band and multiple concentric cluster rings represent the spatial, temporal and clustered information respectively. (b) Time Series Discs, each representing a cluster ring in (a) and formed by multiple triangular HeatMaps. Time sequence is formed by different concentric rings on the disc. There are several obvious warm colored rings on each disc, indicating continously rising tempreture in the selected years. (c) ScatterPlot based on PCA for finding abnormal cases represented by outliers.

Abstract—We present a new approach to visualizing the climate data of multi-dimensional, time-series, and geo-related characteristics. Our approach integrates three new highly interrelated visualization techniques, and uses the same input data types as in the traditional model-based analysis methods. As the main visualization view, Global Radial Map is used to identify the overall state of climate changes and provide users with a compact and intuitive view for analyzing spatial and temporal patterns at the same time. Other two visualization techniques, providing complementary views, are specialized in analysing time trend and detecting abnormal cases, which are two important analysis tasks in any climate change study. Case studies and expert reviews have been conducted, through which the effectiveness and scalability of the proposed approach has been confirmed.

Index Terms—Climate changes, spatiotemporal visualization, station-based observation data, radial layout, visual analytics

1 Introduction

As an important part of natural environment, climate is associated with almost every aspect of our life. According to the IPCC's 4th assessment report [4], global mean air temperature greatly increased after the 1950s, which was most likely because of the rapid increase in the discharge of the greenhouse gases generated in human activities. A series of environmental degradation events caused by climate change have taken place, for example, ocean level rises, extreme weather events occur more frequently, and ecological balance is under threat. Climate changes have received much attention recently, and related studies are conducted worldwide, mostly by international collaborative efforts.

Although climate studies are inherently multi-disciplinary and different domain experts have different views, obtaining continuous, long-term and large-area observation data on land surface is the prerequisite for all studies [52]. Climate data containing multiple parameters, such as air temperature, rainfall, sunshine duration, wind velocity/direction, are usually generated by meteorological stations located in representative regions at regular time intervals, thus the data intrinsically are multi-dimensional, time-oriented and geo-

- *Jie Li is with School of Computer Science and Technology, Tianjin University, and National Ocean Technology Center, Tianjin, China. E-mail: vassilee@tju.edu.cn.*
- *Kang Zhang is with Department of Computer Science, The University of Texas at Dallas, USA. E-mail: kzhang@utdallas.edu.*
- *Zhao-peng Meng is with School of Computer Software, Tianjin University, China. E-mail: zpmeng@tju.edu.cn.*

IEEE Symposium on Visual Analytics Science and Technology 2014
November 9-14, Paris, France
978-1-4799-6227-3/14/$31.00 ©2014 IEEE

related. As the advance of observation techniques, a surface observation network consisting of thousands of stations has been established by the World Meteorological Organization (WMO) and the Global Climate Observation System (GCOS) for climate studies.

Though the techniques used in climate change studies, such as differential equations, could well capture the evolutionary processes of spatiotemporal phenomena, they are costly and have other well-known limitations [10]. For example, most of these techniques attach great importance to the analysis models, while lacking interactive processes and the capability of intuitively analyzing big meteorological data. Individual changes hidden in such statistics-oriented processes are often ignored, when analyzing the overall changes. Furthermore, because a large number of climate problems have no reliable "ground truth" data, it is crucial to develop objective evaluation methods for comparing the outcomes of different analysis techniques. We thus resort to visualization techniques, and attempt to design a visualization framework that can intuitively and interactively reveal the evolutionary nature of climate change patterns at different spatiotemporal scales. We aim at addressing the following requirements [3]. First, climate represents the long-term average meteorological status in given regions, to evaluate climate changes, statistical analyses based on decades or longer observation data are necessary. Second, climate is inherently associated with geo-information, so the visualization granularities between temporal and spatial dimensions must be balanced and easily tuned. Finally, apart from macro and global climate change phenomena, users, such as climate researchers and policy makers, may also be interested in local and micro (e.g. abnormal) conditions.

Our goal is to identify climate change patterns through visual analysis based on in-site climate observation station data which are also essential for traditional quantitative methods. The proposed visualization framework for climate changes, which we will call Vismate, contains three visualization modules, i.e. Global Radial Map, Time Series Discs and Anomalies Detection Scatterplot. To evaluate our approach, we used Vismate to analyze China Surface Data for International Exchange and Global Historical Climate Network (GHCN) [25] data, as shown in Fig. 1 and Fig. 12 respectively. By consulting domain experts and checking against the related literature, all the patterns discovered in our case studies have been confirmed, thus proving the effectiveness and the scalability of our approach.

The major contributions of this paper include:

- Visimate, a visual analytical framework for discovering climate change patterns at different spatiotemporal scales.
- Three complementary visualization techniques for spatial and temporal patterns in a single view, time-series patterns, and anomaly detection.
- Discovery of several temperature patterns of China and the world relating to the climate changes.

The remaining part of this paper is organized as follows. Section 2 reviews related work. The approach overview is then described in Section 3, followed by three complementary visualization techniques in Section 4, 5, and 6 respectively. Section 7 describes two analytical case studies and an expert review. Finally, we conclude the paper in Section 8.

2 Related Work

2.1 Spatial and Temporal Visualization

Thematic map [41] is perhaps the most traditional method of geo-related data visualization, which can be viewed as an overlay of heatmap or glyphs on a map. A novel type of quantitative thematic map was introduced by Speckman et al. [43], i.e. Necklace Maps. Taggram [29] is another type of thematic map, in which tag clouds [26] were plotted on a map to represent the area characteristics. These methods work well for representing static data, but provide limited supports for visualizing time-oriented geographic data. Many researchers attempted to tackle this problem by jointly using a map and other time-series visualization techniques. Malik et al. [27] comprehensively used the map, bar chart, line chart and pie chart to analyze the correlation between urban crime activities and spatiotemporal dimensions. Landesberger et al. [24] designed a dynamic categorical data view (DCDV) to visualize human position transitions in one day, and associated it with a geography view. Furthermore, parallel coordinates [20, 47], ThemeRiver [16, 17], stacked bar charts [30], and even all existing time-series visualization techniques can be combined with a map to form effective spatiotemporal data visualization tools. However, these loosely coupled spatiotemporal visualization methods do not provide an overview of spatial and temporal dimensions, and lack of intuitive and compact methods for visualizing spatiotemporal data in a single view. Different from such multi-view methods, our approach offers a global yet compact view, integrating both the spatial and the temporal features.

Radial visualization, or displaying data in a circular or elliptical layout, is an increasingly common technique in information visualization [6], which often encode time dimension by several concentric rings [2, 50]. However, we often ignore its advantage of representing orientation and position due to its non-directional shape. For example, Qu et al. [34] designed an s-shaped axis used in parallel coordinates to represent the wind direction, and Malik et al. [28] used multiple regular polygons for the comparative visualization. To improve the effectiveness and gain enough space for extra visualization components, one often utilizes the inside and outside of the radial visualizations. For example, Draper et al. [7] put search conditions in the central space, while Wu et al. [50] utilized inside space to place a triangular ScatterPlot. A human body chart was laid in radar plot by Zhang et al. [54] to visualize a person's health condition, and Burch [2] drew many thumbnails outside the outermost ring of the TimeRadar. Inspired by these methods, the main visualization in our framework has also a radial layout. We encode time dimension by different concentric rings along radial direction with a map in the center, so that our approach can visualize spatial and temporal dimension at the same time. Moreover, the outside area of the radial plot is utilized to represent clustered information that is very essential for climate studies.

2.2 Climate Data Visualization

Visualization has been an effective tool in climate studies, and there are many classic visualization methods, such as contour line [49], standard coloration [41], rose diagram [21], etc.. These methods are usually simple and can only show analysis results, lacking interactions and the abilities for discovering the potential knowledge from big climate data. To clarify the use of the visualization techniques in climate studies, Nocke et al. [31] performed a questionnaire with climate researchers. The results showed that traditional 2D visualization techniques were the most widely used tools in climate studies, and there was a gap between climate studies and information visualization techniques. As the advance of information visualization, more climate researchers have applied the state-of-the-art visualization techniques to climate studies. Koethur et al. [22] combined clustering and visualization to capture the prominent spatiotemporal features from environment models. Tominski et al. [48] visualized the global climate network using information visualization techniques. Johansson et al. [19] used a 3D GIS platform to show the climate data. Both Yannier et al. [51] and Janicke et al. [18] have studied how to visualize weather variations, which are similar to our work. Their studies, however, focus on the use of touch screen in enhancing the viewer's perception, which would potentially complement our work.

The most related idea was that of Drocourt et al. [8], which uses a radial layout plus a map to study the changes (advance/retreat) of glaciers in Greenland. Glyphs of different shapes and colors were drawn on the sectors of a circle to represent individual changes. The visualization result, however, is a static picture without any interaction for exploring the detailed information, and the plot can

only accommodate about 200 objects due to the limited angular resolution of a circle. Furthermore, the authors did not discuss how to use this visualization to find the spatiotemporal patterns in other fields, which prevented it from being used as a more general tool.

To our knowledge, no comprehensive information visualization technique specialized in climate changes have been developed, particularly for using the same data as traditional climate studies.

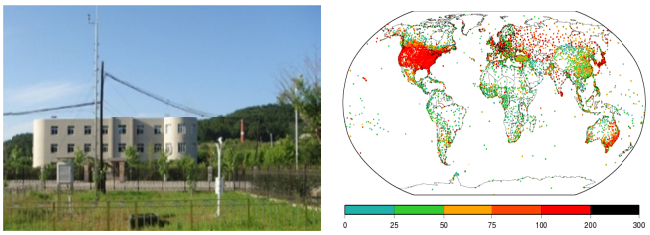

(a) (b)

Fig. 2. (a) A typical meteorological observation station in Dalian, China. (b) The distribution of about 7000 meteorological observation stations in GHCN. Colors represent the number of operating years of the stations.

2.3 Climate Change Study

Climate change studies focus on trend analyses [14], impacts on other fields [32] and response strategies [12], in which model-based methods have been widely used. Many of the latest findings of global climate changes can be found in the IPCC reports [4, 45]. China has also increasingly concentrated on climate changes. Notably, Chinese climate scientists have contributed numerous published scientific findings. These conclusions have specific spatial and temporal characteristics, for example, Ren et al. [37] found that the warming was more evident in Northern China than in the South. Yue et al. [52] draw a time series plot of annual average temperature in China using a novel spatial interpolation, which clearly shows that the warming started from the 1980s. Piao et al. [33] pointed out that precipitation variations do not have significant long-term trends at the national level since 1960, however, there are significant regional patterns. Sun et al. [46] found that the number of cold climate extremes became more moderate, while extremely high temperature events did not significantly increase [36]. Many other important findings have been reported by Ding et al. [5].

A clear trend is that more and more data-driven methods have been applied to climate change studies. Faghmous and Kumar [10] analyzed the practicability of using spatiotemporal data mining in climate data. Steinhaeuser et al. [44] reviewed the progress, opportunities and challenges of using the complex network in climate studies. An important project [23] containing numerous cases of using data-driven methods in climate change studies has been funded by the US NSF Expeditions Program in computing program which is aimed at pushing the boundaries of computer science research. In general, the inter-disciplinary characteristic of climate studies becomes more apparent.

Climate change awareness among the public is also a hot research issue. Schmidt et al. [39] analyzed the media attention for climate changes of 27 countries by comparing the newspaper coverage. Adam et al. [15] studied the variation in the translations of the IPCC's 4th Assessment Report (AR4) [4] "probability expressions" between the Chinese and British publications to reduce the public's misconceptions of the report. Semenza et al. [40] investigated the climate change awareness of the public by telephone interviews, and reported that more than 90% of the people heard of global warming, but only about half of the interviewed have more or less changed their lifestyles to reduce the emissions of greenhouse gases. Although the reduction in greenhouse gas emissions mainly depends on the international and national efforts, gaining the public support is of great importance. A recent survey in the United States [35] confirmed that public opinions on the existence and the importance of global warming strongly depended on their perceptions of recent local climate variations. It is, however, impossible to feel and remember long-term and subtle climate changes for ordinary people. Therefore, more publicity is needed to promote low-carbon life, and the information visualization surely plays a positive role in this aspect.

In summary, although several related studies and projects have been conducted on data analyses of climate changes, little effort has been devoted to the customized design of visual analytics in climate change studies. There is an urgent need for such a visual analytical tool for both professionals and the public, which is the main motivation of our work.

3 Approach Overview

3.1 Data Sources

Our methods analyze land surface observation data, generated mainly by meteorological observation stations (see Fig. 2a), and used in almost every climate change study. Thousands of meteorological stations have been built around the world, operated by different countries and organizations, as shown in Fig. 2b. Due to the automatic observation capabilities of these stations, huge amounts of meteorological observation data are continuously transferred to designated data centers for archiving. We directly use two datasets of such kind as inputs, which contain different numbers of stations and are published on NOAA National Climate Data Center (http://www.ncdc.noaa.gov) and China Meteorological Data Sharing Service System (http://cdc.cma.gov.cn) websites.

3.2 Domain Requirements

To better design the climate visualization framework, we classify the most important tasks of climate change studies into three major categories:

- **Spatial Distribution:** identifying climate changes at different spatial scales, such as continent, zone, country, areas, province and city.
- **Time Series Characteristic:** determining the climate change trends of different areas, highlighting key turning points, and even predicting the future change based on the patterns observed today.
- **Abnormal Case:** discovering the areas that are changed in patterns drastically different from their neighboring areas.

3.3 Visualization Modules

Based on the collected data and the visualization tasks, we have developed a comprehensive climate change visualization framework that contains three modules:

- **Global Radial Map** – a radial layout including a map shows the geospatial distribution. The K-Means clustering algorithm is adapted in this visualization to divide all the stations into a number of groups, each having similar change rates.
- **Time-Series Discs** – multiple time-series triangular HeatMaps around a center point forming a disc, as in Fig. 1b. Each triangular HeatMap encodes the change rate between every pair of years of a station during a pre-defined time interval. Aligning triangles as a disc aims at helping climate experts to compare the time trends and identify important temporal patterns across different stations.
- **Anomaly Detection ScatterPlot** – a slice of a triangle, such as row, column, or hypotenuse could be selected to form a multi-dimensional vector. To detect abnormal cases, one could select any slice from all the triangles to be projected into a scatterplot based on PCA [21].

Of the three modules, the Global Radial Map offers the primary visualization, supplemented by other two modules. These modules have their own strengths and weaknesses, specialized in different

tasks, and one can use either one module separately, or two or three together based on the analytical tasks at hand.

4 Global Radial Map

We believe that full awareness, investigation, and understanding of both time and spatial patterns at the same time is extremely important, and therefore design the Global Radial Map to visualize spatiotemporal patterns in a compact view.

4.1 Map Drawing

To embed a map into a circle, the map's bounding box should fit into the circle. Using the traditional longitude/latitude equidistance grid projection, a world map could be projected onto a rectangle with the width twice of its height, which will waste much space in the circle, as shown in Fig. 3(left). We choose to change the map projection by selecting the Mercator projection [42] featured with shape-preserving after converting a world map to a square within a specified bounding box (longitude:-180°~180°, latitude:-85.05°~85.5°). The phenomenon of area enlargement becomes more serious as latitude increases, and the regions higher than 85.05° and lower than -85.05° cannot be mapped. Such effects on our visualizations are, however, limited due to the area-preserving feature of the Mercator projection and the fact of only one station (Amundsen-Scott South Pole Station) in such a high-latitude area.

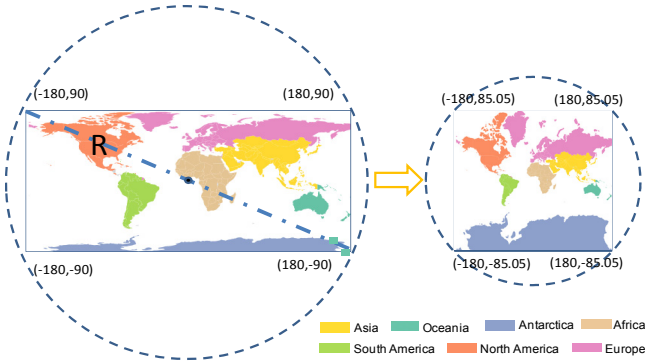

Fig. 3. Comparison of traditional longitude/latitude equidistance grid projection (left) and Mercator projection (right).

Our drawing method not only needs to cater for the world map, it should also be designed as generic as possible to accommodate other geographic shapes of different countries. One of the key problems is to compute the map's central coordinate. Drocourt [8] used a modified standard formula to compute the map gravity center of Greenland. The author, however, has not considered the scale issue and not tested his method on any map having a concave polygon contour. Inspired by GIS platforms, we use several interactive operations, such as pan, zoom-in, zoom-out, etc., to operate maps containing any countries and areas, instead of using complicated algorithms. Through these interactions, users could flexibly explore various geographical areas at any scales in an interactive manner, which is particularly useful for visualizing big data obtained from a huge amount of stations.

To keep the map style intuitive and minimize the viewer's cognitive effort, we use the online tool ColorBrewer [1] to assign a color in the recommended color solution to each area. The selected color solution is also used for spatial mapping (see Section 4.2), in which stations are colored the same as the areas they belong to.

4.2 Spatial Mapping

Mapping each station with longitude, latitude and elevation 3D coordinate to a 1D angular coordinate system creates extra space that could be used to represent time and clustering information. One of the challenges in spatiotemporal mapping is to minimize the loss of spatial information when computing the angular coordinate for each station. The fact that not all the stations are on the contours of any country makes the coordinate transformation more difficult.

To avoid that two geographically distant stations are arranged near each other on the ring, we use a hierarchical mapping strategy, i.e. first divide a map into several subareas and assign an angular span to each subarea in proportion to the number of the stations in that area, and then project the stations in each area onto the ring according to a reference. We use the latitude coordinate of a station as the reference (see Fig. 4b), because climate change is sensitive to the latitude. Having obtained the angular coordinate of the first station in one area, which is equal to the area's starting angle, the angular coordinates of other stations in that area can be determined by simply adding an equal angular interval to the angular coordinate of the previous station to simplify the drawing algorithm and to maintain the symmetry of the visualization, as in Fig. 4a.

Assume P be the set of stations, L be the set of hierarchical levels, and A_i be the set of subareas at the *ith* level. The algorithm of computing the $origin_{i,j}$ and $span_{i,j}$ representing the starting angle and the angular span of the *jth* area in the *ith* level as follows:

Algorithm.1 Determine the origin and span of each subarea

$L = \{l_1, l_2, \ldots, l_N\}$

$A_i = \{a_{i,1}, a_{i,2}, \ldots, a_{i,M}\}$

$origin_{1,1} \leftarrow \max\left(\left\{a \middle| a \text{ is the latitude of each stations in } a_{1,1}\right\}\right)$

For all $l_i \in L$, i>0 do

  For all $a_{i,j} \in A_i$, $l_j \in L$, j>0 do

    $span_{i,j} \leftarrow \frac{360}{|P|} \times |a_{i,j}|$, $|\ |$ represents the station number symbol

    if $j = 1$ then

      $origin_{i,j} \leftarrow origin_{1,1}, i > 1$

    else

      $origin_{i,j} \leftarrow origin_{i,j-1} + span_{i,j-1}, i > 1$

    End if

  End for

End for

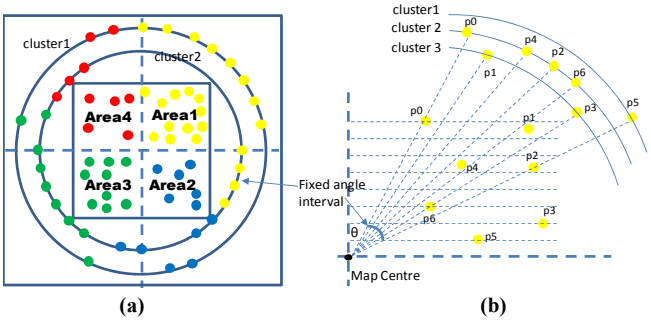

Fig. 4. (a) An example of spatial mapping (the ring band representing time information is omitted); (b) Sorting stations based on their latitudes.

4.3 Temporal Mapping

The Global Radial Map provides sector-based ring plot for displaying raw observation data, offering the visualization of the basic meteorological condition of each station. Radial direction indicates the positive direction of the time axis. Each sector indicates the time series of one station, while a radial bin is colored to represent the concrete attribute value at a time point. Fig. 5a shows a time series visualization example of four years at six stations. Each sector is colored according to the attribute value, and the selected

attribute is also used for clustering, to be discussed in the next subsection. Designing an intuitive and rational color legend is the key to temporal mapping. We use a Chinese meteorological industry standard [53] to define the color codes of multiple meteorological attributes, as depicted in Fig. 5c.

4.4 Clustering

To clearly display the stations experiencing similar climate changes, the Global Radial Map includes multiple cluster rings, each representing a cluster of the stations, as in Fig. 1a and Fig. 5b. Warm and cold colors encode positive and negative average change rates of the cluster respectively. A ring's thickness represents the absolute value of the average slope of linear regression line between time and a meteorological parameter attribute. To support clustering, we first compute the slope to represent the climate change condition of a station. Let $X=\{x1, x2,\ldots, x_N\}$ be the set of time points in the selected time interval, and $Y=\{y1, y2,\ldots, y_N\}$ be the set of a meteorological attribute values at the corresponding time points, and $\bar{x}$ and $\bar{y}$ represent the average value of the X and Y. The slope is calculated as follows:

$$slope = \frac{\sum_{i=1}^{N}\left(\left(x_i-\bar{x}\right)\left(y_i-\bar{y}\right)\right)}{\sum_{i=1}^{N}\left(x_i-\bar{x}\right)^2} \quad (1)$$

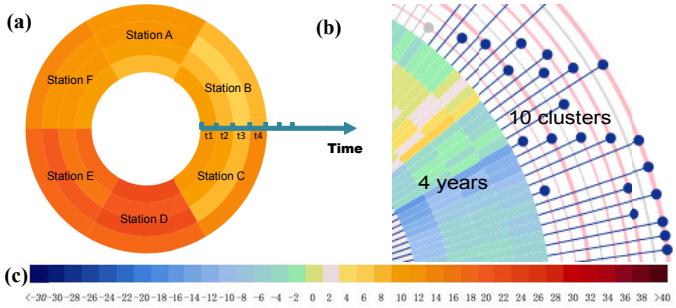

Fig. 5. (a) Temporal mapping represented by a sector-based ring-band. (b) An actual example with 10 cluster rings spanning 4 years. (c) Temperature legend.

4.5 Typical Usage Scenario

When using the approach, the user should first input parameters to draw the Global Radial Map. As shown in Figure 9a, the parameter selection bar contains six parameters, such as the start year, end year, etc.. If the month checkbox is checked, the Global Radial Map will use the month dataset, otherwise the year dataset will be used by default. The number of the clusters can also be selected through a drop-down-list according to the study requirements. Having generated the main view, the system also activates other two views. Moreover, the system can respond to user operations on-the-fly, because the underlying data structure is carefully designed and the data pre-processing procedures have been performed.

4.6 Limitations and Alternative Representations

The current visualization design in Vismate may not best suit all possible scenarios and applications, but could be easily adapted or tailored for different application requirements. For example, as the number of stations increases, angular intervals decrease. Therefore, with a large number of stations, angular intervals are too small to clearly display each station. To solve this scalability problem, we could modify our mapping rules in two aspects. First, rather than assigning an angular coordinate to each station, we can assign it to a group. Second, the points on a cluster ring indicate the number of stations of the group on this cluster.

Using the GHCN data (see Fig. 12) as an example, to accommodate about 7000 stations throughout the world, we can modify the Global Radial Map. We first construct a hierarchical structure of three levels: station, country, and continent. Since the number of the countries in the world is about 200, grouping on countries enable each group to be clearly displayed along the circumference. Consequently, the points on each cluster ring indicate a group of stations in that cluster for the corresponding countries and the sizes of the points encode the number of the stations of the group (to be shown in Fig. 12b). To facilitate spatial search and clearly display the overall state more conveniently, the sector-based ring plot can be replaced by the station search bins representing different sub areas, such as continent, country and province. To visualize the global climate changes, we also add 10 radial bins to indicate the Arctic Zone, North Temperate Zone, Tropic Zone, South Temperate Zone, and Antarctic Zone of Eastern Hemisphere and Western Hemisphere, since climate changes are often associated with the latitude. When the mouse hovers on one bin, the points in the corresponding area will be highlighted in the map, as shown in Fig. 12b. Another possible change is to sort all the cluster rings outward on the average temperature change rates, and thus to display the overall state more clearly.

5 Time Series Discs

To support more detailed time series analysis, we provide a specialized visual analytical tool, called *Time Series Discs*.

5.1 Basic Triangular Component

The basic component of a Time Series Disc is a triangular HeapMap, as shown in Fig. 6a. Each triangle represents a station's changes in a pre-defined time interval. The x-axis of the triangle represents the end year, while the y-axis represents the start year. Each small rectangle in the triangle is colored to represent the change rate, computed by Equation 1, from a start year (x coordinate) to an end year (y coordinate). Color distributions along a specific direction could convey interesting patterns among multiple small rectangles. Fig. 6(b-e) shows four important usages, each corresponding to a specific slice of the triangle:

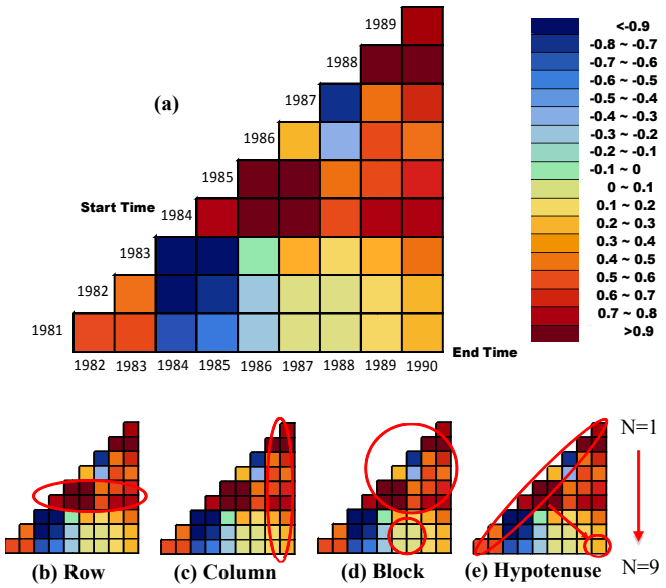

Fig. 6. A triangular component of Time Series Discs. (a) A yearly marked triangle. (b-e) Four important ways for reading the triangle.

- **Row** - each row encodes the changes from a year to every other year. A similar color distribution in one row represents a

continuous and consistent change from that year to later years, as in Fig. 6b. Rows offer the most important view, particularly when multiple triangles are bundled together to form a disc (see Section 5.2).

- **Column** - each column encodes the changes from all the previous years to the year represented by this column. Similar to the "row", a consistent color distribution in a column indicates a minima year (cool color) or a maxima year (warm color). In Fig. 6c, the overall temperature had risen in the 1980s, because all the small rectangles in the column of 1990 are in warm colors, and 1984 had the minimal yearly average temperature, because the change rates from 1984 to all other years are positive and those from the previous years to 1984 are all negative.
- **Block** - a block refers to several nearby rectangles. When having similar colors, the rectangles in a block indicate similar climate conditions in the years represented. A special type of block is sub triangles, which represent stable and consistent changes in the covered years. The example in Fig. 6d reveals that the temperatures in 1987 and 1988 are almost equal, because the change rates from other years to these two years are almost the same (see the small block), and the selected sub triangle shows that the overall warming started in the mid-1980s.
- **Hypotenuse** - each triangle may be considered a number of incremental triangles started from a single rectangle and thus has multiple hypotenuses. The hypotenuse increases from inside to the longest for the entire triangle. Each hypotenuse indicates a year-to-year change of N-years average change rate, where N is the hypotenuse's ordinal, as in Fig. 6e. For example, the 1st (longest) hypotenuse represents the continuous year-to-year temperature change from 1981 to 1990, and the 2nd hypotenuse indicates the year-to-year change of 2-years average change rates. As the increase of the ordinal, occasional changes in that period are averaged out such that the overall state becomes clearer. The shortest hypotenuse having only one rectangle indicates the average change rate over the entire 10 years. Fig. 6e reveals that the overall temperature had risen in the 1980s, while average change rates in the 1980s were about 0.2~0.3.

5.2 Rotating Triangles

Although the time-series triangle can be used to detect the temporal patterns of a station, in many cases one wishes to know the overall change of an area. We therefore construct a radial layout like a disc by aligning the triangles representing multiple stations around a center (see Fig. 7b), through which users could observe and compare climate changes of the stations. We also associate a time series plot with each station. When the user clicks on a triangle, a linear regression analysis is performed on the clicked station, and the regression line is drawn in the time series plot, as shown in Fig. 7c. Users can also add breakpoints to the time series by selecting the CheckBoxes under the time axis, and view the regression line of each individual interval. Fig. 7c shows an example of regression line with 4 breakpoints (1984 and 1985, while 1981 and 1990 as the start and the end years are selected by default). By observing the fitting degrees of the regression lines, the user could immediately view the homogeneity of each interval and choose a more accurate division solution having the smallest residuals over all the intervals. Such an interactive support could significantly improve the precision of regression analysis. We also provide a toolbar for the user to select stations and manipulate the time series plot (see Fig. 7a). Comparing with traditional time series analysis methods for meteorological data, our method could interactively show the analysis process and help users quickly grasp the change trends of any temporal intervals.

6 Anomaly Detection ScatterPlot

Apart from the global climate change trend, local abnormal cases are also the research hotspots. For example, though the air temperature in China has been increasing since the 1950s, Sichuan province has a significant downward trend, which has inspired the scientists' interests. Therefore we need a specialized tool to clearly show the abonormal cases among all the stations during the entire range based on a flexible anomaly detection model.

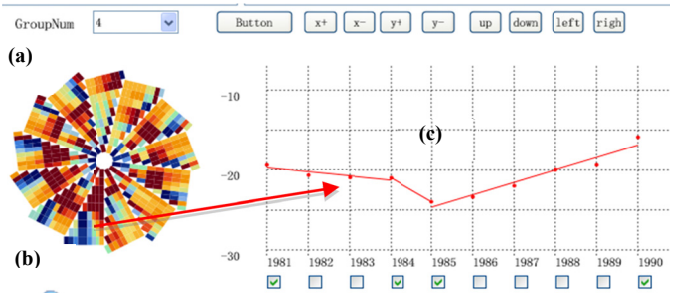

Fig. 7. (a) Toolbar for selecting a cluster in the Global Radial Map (not shown here) and for operating the time series plot. (b) A Time Series Disc. (c) The interactive time series plot for a selected station.

Since a matrix illustrating the climate change rate between any two temporal points of a station has been constructed in a triangle (lower triangular matrix), it is convenient to use the matrix as the foundational data structure. A similar method, extracts the similarity matrix to detect the temporal similarity in field data [9]. Any slice of each triangle, such as row, column or hypotenuse, can be selected as a high-dimensional vector. We use the Principal Component Analysis algorithm (PCA) [21] to map a corresponding slice in all triangles to a point in two-dimensional Cartesian Coordinates. To reveal the correlation between a spatial dimension and its PCA projection, we provide a box query and when selected, and the Global Radial Map automatically highlights the selected stations in the ScatterPlot, as shown in Fig. 8. Through this visualization, one could easily identify outlier stations and also observe similar climate changes among nearby points in the scatterplot.

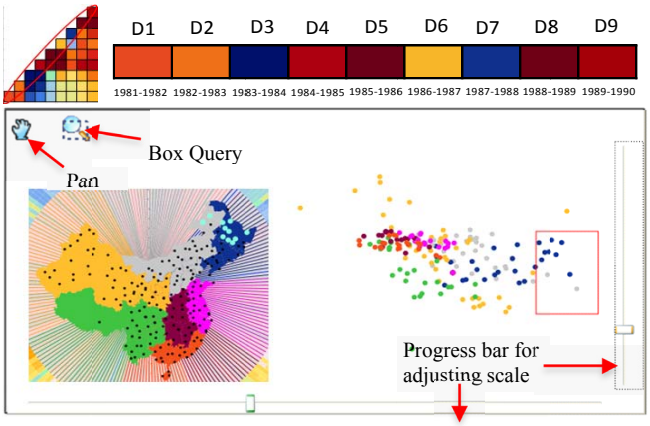

Fig. 8. Anomaly Detection ScatterPlot based on PCA. A hypotenuse slice is selected as the 9-Dimensional vector of each station for mapping.

7 Evaluation

This section reports our evaluation of Vismate through two case studies in different spatiotemporal scales.

7.1 China Surface Data for International Exchange

China surface data for international exchange contains the long-term observation records of representative 206 stations distributed throughout the country. Within the China meteorological observation network, these stations could automatically and continuously obtain 23 types of meteorological attributes on the land surface. The dataset covers 1951-2012, containing about 4 million daily average records,

135000 monthly average records and 47000 yearly average records. The entire set has been checked for consistency by the meteorological authority, and thus is reliable to use.

We first divided China into 7 areas using the customary geographical division method in climate studies, and assign a color to each area, as in Section 4.1. Monthly average data and yearly average data are used, as climate refers to long-term and macro meteorological conditions. If a microscopic meteorological phenomena needs to be analyzed, daily average analysis is also supported by our approach.

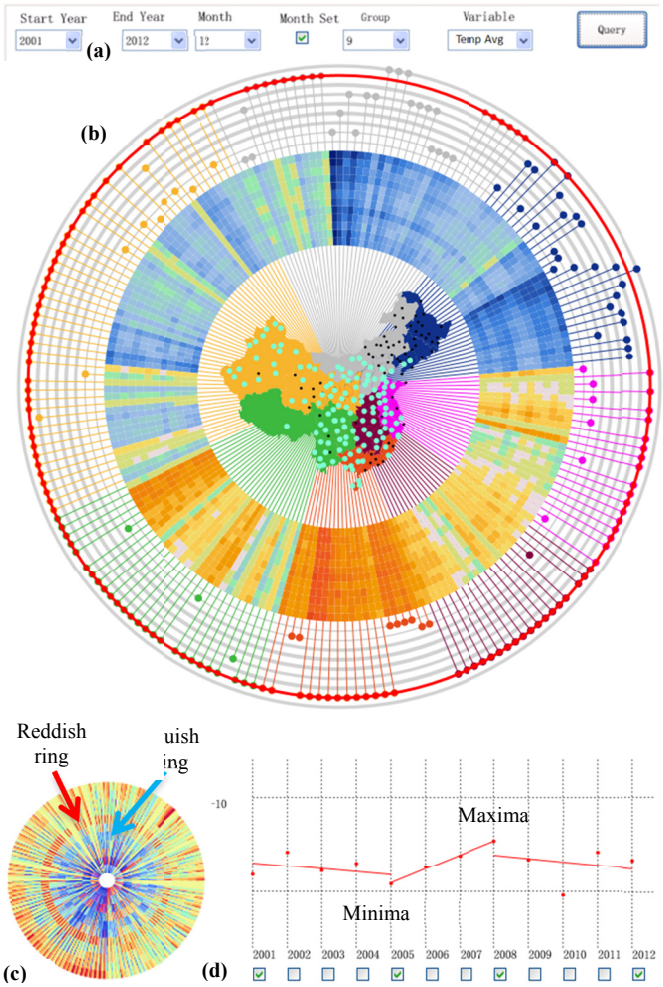

Fig. 9. The winter climate change in China during the period of 2001-2012. (a) The parameter selection bar. (b) Most of the stations are in the selected cluster ring showing a slowly rising trend. (c) A reddish ring and a bluish ring in the Time Series Disc represent a minima point and a maxima point respectively, and (d) the time series plot also proves this finding.

7.1.1 Verifying the Existing Conclusions

To test the effectiveness of Vismate, we first verified a few existing conclusions that had been proven. Using the example of Fig. 1, the interval from1975 to 1989 is recognized as the period when China's climate change happened. We divided the stations into eight clusters according to the temperature change rates using the K-Means algorithm. Two of the clusters have decreasing trends, while others have obvious increasing trends, indicating an overall warming trend during that period. When selecting the cluster ring 6 (second outmost ring) that has a decreasing trend, we found that the all the stations in Sichuan province (highlighted in green area) had distinctive decreasing trends, exactly as reported in Ren et al. [37]. By visualizing the time series of this cluster containing most of the stations using a Time Series Disc, we found that the stations near the centers were all reddish, indicating a continuous temperature rise. This is consistent with the conclusion that the national warming began in the mid-1980s, and there was no significant climate change trend before then [37]. Many other conclusions can also be found using Vismate, such as, climate warming continues in the 1990s, 1998 is the hottest year in history, and the temperatures rise in the winter is more severe than in other seasons.

7.1.2 Interesting Findings

We first used month average records to analyze the **overall climate change** in the winter during the period of 2001-2012. When all the stations were mapped on the cluster rings, spatiotemporal patterns were clearly shown. In Fig. 9b, the reddish ring represents the selected cluster, and all the stations in this cluster are also highlighted in the map, showing that this cluster contains most of the stations, except Northeast China and the northern part of North China. An interesting finding is that all of the rings, except the selected one, reveal various degrees of decline trends, which is different from our expected results. We thus used the corresponding Time Series Disc to obtain a detailed view.

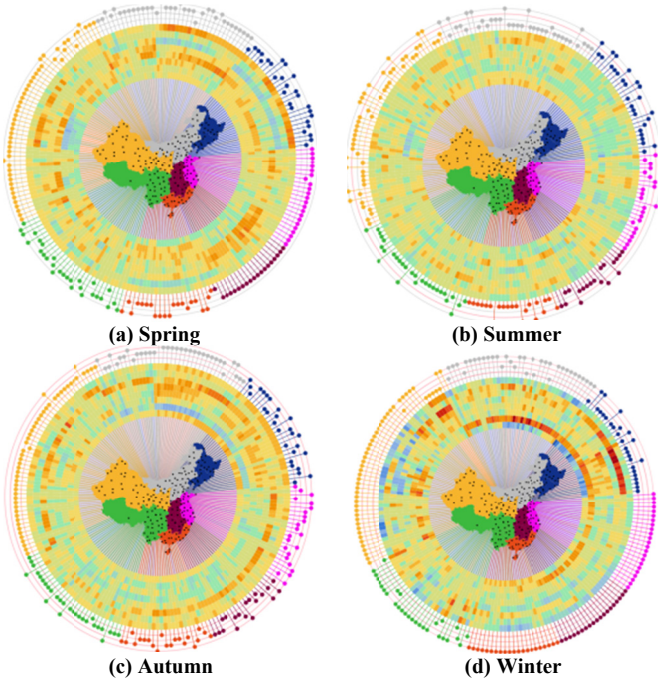

Fig. 10. Seasonal climate changes during the period of 2001-2012.

Fig. 9c displays the time series analysis of Cluster 6 containing most of the stations. Despite a large number of the stations in this cluster with little room to clearly display each small triangle, temporal patterns can still be observed. There are two circles, warm colored and cool colored, representing a minima point and a maxima point respectively, using the "Row Pattern" (See Section 5.1). By mouse interactions, we found the corresponding two years being 2005 and 2008. We also randomly selected other stations and viewed their time series plots, which also showed the same results, as in Fig. 9d. Similar patterns can also be found in other clusters. Therefore we drew the conclusions that temperature continued to rise in the 2000s, yet since 2010, the temperature changes have been showing a downward trend. Climate researchers provided their interpretation: the downward trend in recent years cannot change the fact of global warming, and are only viewed as a normal fluctuation.

Seasonal climate changes are also of interest to researchers. Although the seasonal change patterns before 2000 have been published [45], few have analyzed the seasonal variation patterns in recent years. To fill this gap, we used Vismate to visualize the temperature anomalies in different seasons, as shown in Fig. 10.

Warming trend in the winters was very strong, especially in Northeast China (see the dark red sectors in Fig. 10d). Spring and autumn also had obvious warming trends, and in East China such trend was even more obvious than in the winter. The warming trend in the summer was the weakest. We found that the overall seasonal variations in the 2000s were the same as the prior years. Climate academics confirmed our findings by stating that seasonal climate changes have stable characteristics that do not suddenly change.

We selected the "hypotenuse slice" for each station as an 11-Dimensional (2001-2012) vector, and used the **Anomaly Detection ScatterPlot** to find the stations having abnormal year-to-year climate changes. As shown in Fig. 11a, there is a station in Northeast China (blue) far away from other mapped points. We selected this station to view the corresponding time series plot (Fig. 11b), and found that this station had an opposite change process (2008 had a minima point and 2005 had a maxima point). This example demonstrates the effectiveness of Vismate in finding unusual cases.

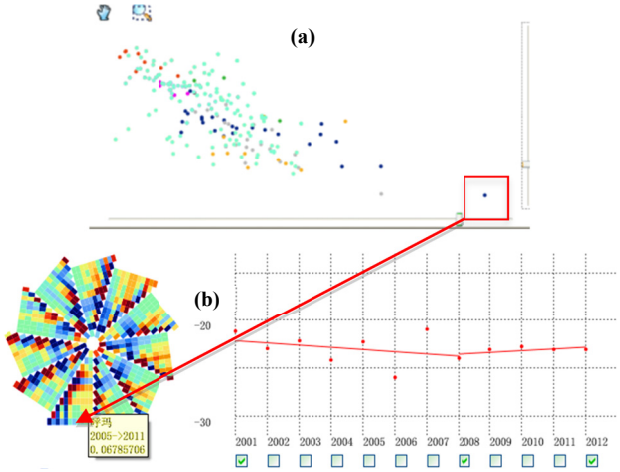

Fig. 11. (a) Anomaly Detection ScatterPlot with an outlier. (b) The corresponding time series plot.

7.2 Global Historical Climate Network (GHCN) Data

The Global Historical Climatology Network (GHCN) temperature dataset is one of the most important datasets for the study of the world's historical climate changes. This dataset is gathered from over 7000 meteorological observation stations throughout the world, which have different start years and end years from 1701 to 2010. Because this dataset only contains records before 2010, and few (only 15.4%) stations have records during the 2000s, we report our findings during the period of 1981-1989 as in Fig. 1, which also serves to compare the global climate changes with China's changes during the same period. We selected monthly average records of December as our analysis objects to demonstrate the effectiveness of Vismate. To accommodate large amounts of stations, we made several representational changes to the Global Radial Map, as described in Section 4.5.

We divided all the stations into 9 clusters (5 warming and 4 cooling), as in Fig. 12a. By viewing the station distributions on each ring, we found that global warming was much stronger in Asia than in other areas of the world, because the stations in China are all red (see Fig.12c), while only the stations in the northwest of America are red (see Fig. 12b). We also observed that the global warming started in the 1980s, which was consistent with the situation in China. Most of the stations in China had rising trends, indicating a stronger warming change in China than the global average change, as in Fig. 12c. The variations in the populated Northern Hemisphere were higher than in Southern Hemisphere, demonstrating that human activities caused climate changes to some degree [45]. However, North America was an exception, in which most stations had cooling trends except in the northwest. Surface Temperature Analysis system [55] of Goddard Institute for Space Studies (GISS) was used to verify our findings. We selected the same temporal interval, and the model-based system outputs the same result as what Vismate showed, as in Fig. 13.

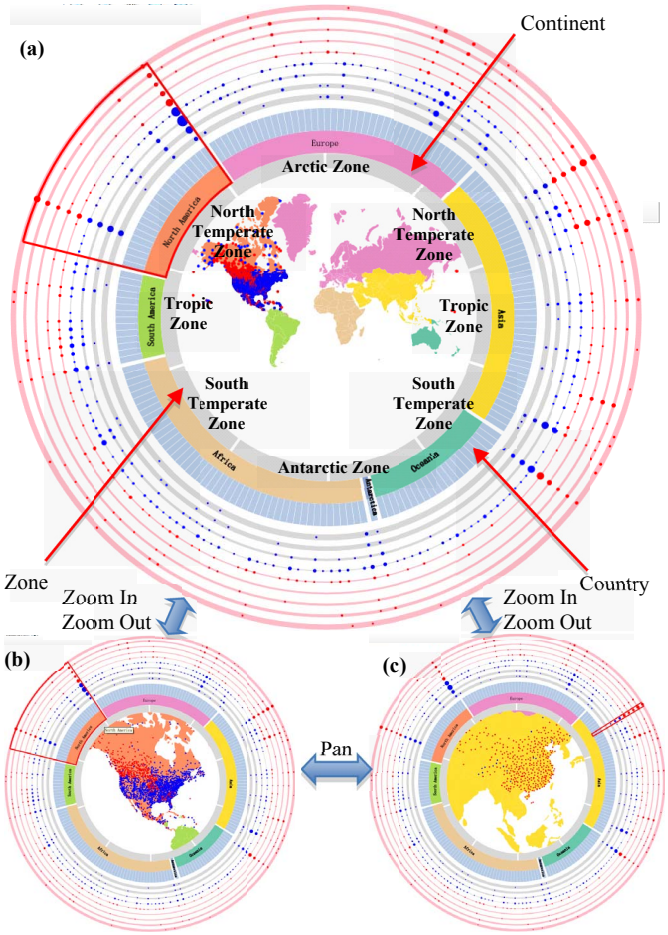

Fig. 12. The Modified Global Radial Map. (a) The climate changes of North America during the period of 1981-1989. (b) North America in a higher scale. (c) A general warming trend in China.

7.3 Expert Review

We have conducted an expert review with fifteen experts from the National Ocean Technology Center and Naval Marine Hydrometeorology Center participated in our evaluation. The selected experts have different disciplinary backgrounds, and are all members of the "Investigation into the Effects of Ocean-Atmosphere Interactions on Global Climate Change" project. Four of the experts are female, while others are male. The ages of most experts are between 30 and 50 (one under 30, and two over 50), and the average age is 37.93.

We first explained our approach and the prototype system to the experts. After getting familiar with the system, they were asked to complete our questionnaire by providing scores between 0 and 10 on seven aspects: aesthetics, visual design, interaction, learnability, performance, functionality, and scalability. We did not impose the time limit, yet every questionnaire was completed within two minutes. Table 1 shows the statistical results of the expert review.

The results show that the average score of *aesthetics* is the highest and the variance is also the smallest, since almost all the experts liked the design of graphical user interface and visualization. The *visual design* aspect was also scored relatively high, because most of the experts believed that the visual design of the three views were suitable for analyzing domain tasks, and many patterns could be found using the system. All the experts were satisfied with the

scalability aspect of our system, because our approach is generic and applicable to the study of climate changes in other parts of the world, and can accommodate almost any number of observation stations. Furthermore, the experts believe that our techniques are also applicable to many other fields, such as ocean, air quality, earthquake, etc., in which fixed observation stations are widely used to automatically collect long-term data. In particular, the correlations among the three views won praises from the experts. However, two experts with computer science backgrounds pointed out that the response time of map operations was slower than the existing GIS platforms, which affected the score of the *interaction* aspect.

Table 1. Expert Review Result

Factor	Highest	Lowest	Average	Variance
Aesthetics	10	9	9.53	0.27
Visual Design	10	7	8.33	0.52
Interaction	10	6	7.93	1.07
Learnability	9	5	7.07	1.35
Performance	8	6	7.53	0.41
Functionality	9	7	7.87	0.41
Scalability	10	7	8.27	0.64

Although the effectiveness of the three views was confirmed by the experts, several experts advised us to add more professional and visual functions to the system. They even expressed strong interest to see our enhanced version as soon as possible, which was measured by *functionality* aspect. To improve the *performance*, the system contains a pre-processing process, i.e. all the time-consuming algorithms, such as clustering, are done before the system starts. System operations can therefore be responded in real-time. After optimization, the data pre-processing time has been reduced to less than 30s. However, the score of *performance* aspect is not as high as we expected, mainly because the experts overlooked the amount of the data manipulated by the system and expected a high system performance. The *learnability* aspect received the lowest score and highest variance, implying that not everyone can quickly learn the tool. This may be because the learning time is too short for them to get familiar with the system and operate smoothly. Using two different representation schemes in the Global Radial Map may have also hindered quick learning.

The experts also pointed out an important limitation of our approach: "climate change is a complicated process, affected by many factors; although what we discovered have been verified, we cannot guarantee the correctness of our future findings without considering other factors". However, all the existing models output results with inherent uncertainties, because of our incomplete understandings of many physical processes and the fact that not all the meteorological physics have been scientifically modeled. Even opposite conclusions were often drawn by different meteorologists and organizations. For example, as three of the most important climate change study organizations, NASA Goddard Institute for Space Studies (GISS) and NOAA National Climate Data Center (NCDC) consider 2005 as the warmest year, while based on HadCRUT dataset compiled by Hadley Centre of the UK Met Office, 1998 is viewed as the warmest year [13]. So the climate science community often relies on multi-approach ensembles to mitigate the uncertainty that any single model might have. For instance, IPCC used multi-model ensembles to present its assessment of future climate changes [4]. We therefore hope that Vismate capable of objectively visualizing actual observation data can be an effective alternative for experts to verify the conclusions generated by other methods. Vismate may also guide experts in more in-depth studies based on the patterns found in our approach, as a mechanism for hypotheses generation [11].

In summary, Vismate received very positive feedback from the domain experts. Our findings were beyond their expectations, and they never thought of applying information visualization techniques in the traditional meteorology field. Although only air temperature was analyzed in the paper, other attributes can also be visualized in a similar fashion.

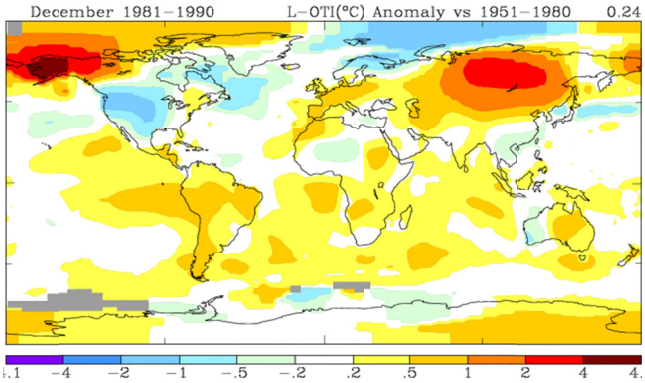

Fig. 13. Goddard Institute for Space Studies (GISS) Surface Temperature Analysis system showing the same changes as in Vismate.

8 Conclusion And Future Work

This paper has presented a comprehensive visualization approach called *Vismate* for climate change studies. New visualization techniques have been developed and integrated into our approach. Vismate has been used to analyze the China Surface Data for International Exchange and GHCN data. Having verified the patterns found in such two datasets, we consider our approach to be effective and useful in real-world scenarios. Furthermore, our approach can be considered general for the visualization of different domain datasets generated by a large number of observation stations, such as ocean, air quality, earthquake, etc.. In the future, we plan to improve Vismate in two aspects. First, we plan to support NetCDF grid data [38] which has been widely used in climate studies. Second, we will utilize the global Re-Analysis data to compare the ocean climate changes with that on the land.

Acknowledgments

The authors wish to thank Zhao Xiao, Zhuang Cai, Meng-Yao Chen, and Chao Wen for their discussions. We are also grateful to the anonymous reviewers for their insightful comments that have helped us in improving the final presentation. This work was supported by Tianjin "Big Data Algorithms and Applications" project.

References

[1] C. A. Brewer and M. A. Harrower. ColorBrewer 2.0: color advice for cartography. Http://colorbrewer2.org/, Penn State University, 2009.

[2] M. Burch and S. Diehl. TimeRadarTrees: Visualizing dynamic compound digraphs. Computer Graphics Forum, 27(3):823–830, 2008.

[3] N. Cressie, C. K. Wikle. Statistics for Spatio-temporal Data. John Wiley & Sons, 2011.

[4] CW Team. Climate Change 2007: Synthesis Report. Contribution of Working Groups I, II and III, to the Fourth Assessment Report. Intergovernmental Panel on Climate Change (IPCC'2007), 2007.

[5] Y. H. Ding et al. China's National Assessment Report on Climate Change. China Science Press, Beijing, 2007. (in Chinese)

[6] G. Draper, Y. Livnat, and R. F. Riesenfeld. A survey of radial methods for information visualization. IEEE Trans. Vis. Comput. Graph. 15(5): 759–776, 2009.

[7] G. Draper, R. F. Riesenfeld. Who votes for what? a visual query language for opinion data. IEEE Trans. Vis. Comput. Graph. 14(6): 1197–1204, 2008.

[8] Y. Drocourt, R. Borgo, K. Scharrer, T. Murray, S. I. Bevan, and M. Chen. Temporal Visualization of Boundary-based Geo-information Using Radial Projection. Computer Graphics Forum, 30(3): 981-990, 2011.

[9] S. Frey, F. Sadlo, T. Ertl. Visualization of Temporal Similarity in Field Data. IEEE Trans. Vis. Comput. Graph. 18(12): 2023-2032, 2012.

[10] J. H. Faghmous, V. Kumar. Spatio-temporal Data Mining for Climate Data: Advances, Challenges, and Opportunities. Data mining and knowledge discovery for big data. Springer Berlin Heidelberg, pages 83-116, 2014.
[11] R. Fuchs, J. Waser, and M. E. Groller. Visual Human+Machine Learning. IEEE Trans. Vis. Comput. Graph, 15(6): 1327-1334, 2009.
[12] L. Gaudard, M. Gilli, and F. Romerio. Climate change impacts on hydropower management. Water Resources Management, 27(15): 5143-5156, 2013.
[13] J. Hansen, R. Ruedy, M. Sato. Global surface temperature change. Reviews of Geophysics, 48(4), 2010.
[14] J. Hansen, M. Sato, and R. Ruedy. Perception of climate change. In Proceedings of the National Academy of Sciences, 109(37): 2415-2423, 2012.
[15] A. J. L. Harris, A. Corner, and J. Xu. Lost in translation? Interpretations of the probability phrases used by the Intergovernmental Panel on Climate Change in China and the UK. Climatic change, 121(2): 415-425, 2013.
[16] S. Havre, B. Hetzler, and L. Nowell. Themeriver: Visualizing theme changes over time. In Proceedings of the IEEE InfoVis'2000, pages 115-123, 2000.
[17] S. Havre, E. Hetzler, P. Whitney, and L. Nowell. ThemeRiver: Visualizing thematic changes in large document collections. IEEE Trans. Vis. Comput. Graph. 8(1):9–20, 2002.
[18] H. Janicke, M. Bottinger, U. Mikolajewicz, and G. Scheuermann. Visual exploration of climate variability changes using wavelet analysis. IEEE Trans. Vis. Comput. Graph. 15(6):1375-1382, 2009.
[19] J. Johansson, T. S. Neset, B. O. Linner. Evaluating climate visualization: an information visualization approach. In Proceedings of the International Conference on Information Visualization (IV'2010), pages 156-161, 2010.
[20] S. Johansson and M. Jern. GeoAnalytics visual inquiry and filtering tools in parallel coordinates plots. In Proceedings of the 15th Annual ACM International Symposium on Advances in Geographic Information Systems, pages 33, 2007.
[21] N. Kambhatla and T. K. Leen. Dimension reduction by local principal component analysis. Neural Computation, 9(7):1493–1516, 1997.
[22] P. Koethur, M. Sips, J. Kuhlmann, and D. Dransch. Visualization of Geospatial Time Series from Environmental Modeling Output. In Proceedings of the EuroVis, pages 115-119, 2012.
[23] V. Kumar. Exceptions in computing: understanding climate change – a data driven method. Http://climatechange.cs.umn.edu/index.php, 2010.
[24] T. von Landesberger, S. Bremm, N. Andrienko, G. Andrienko, and M. Tekusov. Visual analytics methods for categoric spatio-temporal data. In Proceedings of the IEEE VAST'2012, pages 183-192, 2012.
[25] J. H. Lawrimore, M. J. Menne, B. E. Gleason. An overview of the Global Historical Climatology Network monthly mean temperature data set, version 3. Journal of Geophysical Research: Atmospheres (1984–2012), 116(D19), 2011.
[26] B. Lee, N. H. Riche, A. K. Karlson, and S. Carpendale. Sparkclouds: Visualizing trends in tag clouds. IEEE Trans. Vis. Comput. Graph. 16(6): 1182-1189, 2010.
[27] A. Malik, R. Maciejewskiet, Y. Jang, and W. Huang. A correlative analysis process in a visual analytics environment. In Proceedings of the IEEE VAST'2012, pages 33–42, 2012.
[28] M. M. Malik, C. Heinzl, and M. E. Groeller. Comparative Visualization for Parameter Studies of Dataset Series. IEEE Trans. Vis. Comput. Graph. 16(5):829-840, 2010.
[29] D. Q. Nguyen and H. Schumann. Taggram: Exploring geo-data on maps through a tag cloud-based visualization. In Proceedings of the International Conference on Information Visualization (IV'2010), pages 322–328, 2010.
[30] T. Nocke, H. Schumann, U. Bohm. Methods for the visualization of clustered climate data. In Computational Statistics, 19(1): 75-94, 2004.
[31] T. Nocke, T. Sterzel, M. Bottinger and M. Wrobel. Visualization of climate and climate change data: An overview. In Digital Earth Summit on Geoinformatics, pages 226-232, 2008.
[32] P. Pall, T. Aina, D. A. Stone, P. A. Stott, T. Nozawa, A. G. J. Hilberts, D. Lohmann, and M. R. Allen. Anthropogenic greenhouse gas contribution to flood risk in England and Wales in autumn 2000. Nature, 470(7334):382-385, 2011.
[33] S. Piao, P. Ciais, Y. Huang, Z. Shen, S. Peng, J. Li, L. Zhou, H. Liu, Y. Ma, Y. Ding, P. Friedlingstein, C. Liu, K. Tan, Y. Yu, T. Zhang, and J. Fang. The impacts of climate change on water resources and agriculture in China. Nature, 467(7311): 43-51, 2010.
[34] H, Qu, W. Y. Chan, A. Xu, K. L. Chung, and P. Guo. Visual analysis of the air pollution problem in Hong Kong. IEEE Trans. Vis. Comput. Graph. 13(6): 1408–1415, 2007.
[35] B. G. Rabe and C. P. Borick. Fall 2011 national survey of American public opinion on climate change. Issues in Governance Studies, 2012.
[36] S. Rahmstorf and D. Coumou. Increase of extreme events in a warming world. In Proceedings of the National Academy of Sciences, 108(44): 17905-17909, 2011.
[37] G. Ren, Y. Ding, Z. Zhao, Z. Zheng, T. Wu, G. Tang and Y. Xu. Recent progress in studies of climate change in China. Advances in Atmospheric Sciences, 29: 958-977, 2012. (In Chinese)
[38] R. Rew, G. Davis. NetCDF: an interface for scientific data access, Computer Graphics and Applications, 10(4): 76-82, 1990.
[39] A. Schmidt, A. Ivanova a, and M. S. Schafer. Media attention for climate change around the world: A comparative analysis of newspaper coverage in 27 countries. Global Environmental Change, 23:1233-1248, 2013.
[40] J. C. Semenza, D. E. Hall, D. J. Wilson, B. D. Bontempo, D. J. Sailor, and L. A. George. Public perception of climate change: voluntary mitigation and barriers to behavior change. American Journal of Preventive Medicine, 35(5): 479-487, 2008.
[41] T. A. Slocum, R. B. Mcmaster, F. C. Kessler, and H. H. Howard. Thematic Cartography and Geographic Visualization 3nd Ed. Pearson Education, 2009.
[42] J. P. Snyder. Map projections—a working manual (US geological survey professional paper 1395). United States Government Printing, 1987.
[43] B. Speckmann and k. Verbeek. Necklace maps. IEEE Trans. Vis. Comput. Graph. 16(6): 881-889, 2010.
[44] K. Steinhaeuser, N. V. Chawla, A. R. Ganguly. Complex Networks in Climate Science: Progress, Opportunities and Challenges. In Proceedings of the Conference on Intelligent Data Understanding, pages 16-26, San Francisco, CA, NASA, 2010.
[45] T. F. Stocker, Q. Dahe, and G. K. Plattner. Climate change 2013: the physical science basis. Working group I contribution to the fifth assessment report of the intergovernmental panel on climate change. Intergovernmental Panel on Climate Change (IPCC'2013), 2013.
[46] J. Q. Sun, H. J. Wang, and W. Yuan. Decadal variability of the extreme hot event in China and its association with atmospheric circulations. Climatic and Environmental Research, 16(2): 199-208, 2011.
[47] C. Tominski, J. Abello, and H. Schumann. Axes-based visualizations with radial layouts. In Proceedings of the 2004 ACM Symposium on Applied Computing (SAC'04), pages 1242–1247, 2004.
[48] C. Tominski, J. F. Donges, and T. Nocke. Information visualization in climate research. In Proceedings of the International Conference on Information Visualization (IV'2011), pages 298-305, 2011.
[49] D. F. Watson. Contouring. Pergamon Press, 1992.
[50] Y. Wu, F. Wei, S. Liu, N. Au, W. Cui, H. Zhou, and H. Qu. OpinionSeer: interactive visualization of hotel customer feedback. IEEE Trans. Vis. Comput. Graph. 16(6): 1109–1118, 2010.
[51] N. Yannier, C. Basdogan, S. Tasiran, and O. L. Sen. Using haptics to convey cause-and-effect relations in climate visualization. IEEE Trans. Vis. Comput. Graph. 1(2): 130-141, 2008.
[52] T. X. Yue, N. Zhao, R. D. Ramsey, C. L. Wang, Z. M. Fan, C. F. Chen, Y. M. Lu, and B. L. Li. Climate change trend in China, with improved accuracy. Climatic Change, 120:1-15, 2013.
[53] M. Zhang. Color code for products of weather forecast and service GB. Chinese meteorological industry standard, 2009. (In Chinese)
[54] Z. Zhang, B. Wang, F. Ahmed, I.V. Ramakrishnan, R. Zhao, A. Viccellio, and K. Mueller. The Five W's for Information Visualization with application to healthcare informatics. IEEE Trans. Vis. Comput. Graph. 19(11): 1895–1910, 2013.